Novel Compact and Broadband Frequency-Selectable Rectennas for A Wide Input-Power and Load Impedance Range

Chaoyun Song, *Member, IEEE*, Yi Huang, *Senior Member, IEEE*, Paul Carter, Jiafeng Zhou, Sumin Joseph and Gaosheng Li, *Member, IEEE*

***Abstract*—Wireless power transfer (WPT) and wireless energy harvesting (WEH) using rectennas are becoming an emerging technology. This paper presents a novel design method for a rectenna suitable for a wide range of selectable operating frequency band, input power level and load impedance. Most importantly, it is realized without using complex impedance matching networks which shows significant advantages over existing rectennas in terms of the structure and cost. A rectenna example has been designed, made and tested using this novel method. The proposed rectenna has a compact size of 90 × 90 × 1.58 mm^3 and operates at four different frequency bands that are selectable from 1.1 to 2.7 GHz. Over 60% (up to 85%) energy conversion efficiency is achieved for the input power from 0 to 15 dBm and load impedance between 700 and 4500 Ω. The rectenna shows excellent performance for the target applications (WPT and WEH) with a much-simplified structure and reduced cost.**

***Index Terms*—Broadband rectenna, frequency-selectable, matching network elimination, wireless power transfer, wireless energy harvesting.**

I. Introduction

Wireless power transfer (WPT) from a source to a load without the connection of electrical conductors was first demonstrated by Tesla in the 1890s and has been continuously investigated by researchers over the past decades [1]. Nowadays, the development of WPT is of great significance to the modern industry, since a range of potential applications have been found in such as wireless chargers [2], [3], electric vehicles (EVs) [4]-[7], wireless communications [8], sensor networks [9], RFID [10], [11], Machine-to-Machine (M2M) [12], and the Internet of Things (IoT) [13]. In addition to the well-studied inductive power transfer system, the radiative WPT system and the wireless energy harvesting (WEH) from ambient electromagnetic fields using rectifying-antennas (*rectennas*) have become an extremely hot research topic in the recent years [14], [15]. Especially with the upcoming new technology wave of smart home, smart cities and the IoT, self-sustainable standalone low power electronics devices (e.g., smart sensors and monitors) that automatically collect and report the data to the server could play an important role [16]. The WEH would become one of the cutting edge solutions for providing continuous power to low power sensors and monitors.

Much progress on rectennas for WPT and WEH has been made [17]-[27]. Among them, multiband and broadband rectennas with good/excellent performance (e.g., high conversion efficiency and reduced nonlinear effect) have shown significant advantages over other types of rectennas in terms of the output power level and suitability for different operating conditions. However, the optimal design of such rectennas is still challenging due to the nonlinearity of the system. So far, there have been very few multiband and broadband rectennas reported with excellent performance [21], [23]-[27].

Up to now, two widely adopted configurations for multiband and broadband rectennas have been reported, as depicted in Figs. 1(a) and (b). The first configuration is a rectenna using a single branch multiband or broadband impedance matching network and a corresponding rectifier [17], [18]. The signals received by the antenna over the frequency band of interest (from f_0 to f_N) can be delivered to the rectifier through the network. The RF power of the signal is then converted to DC power and delivered to the load. However, there are two major drawbacks of this configuration:

1) The loss of the complete matching network is quite high due to the large number of cascaded circuit components. Thus it would be difficult to achieve a high efficiency rectenna covering different frequency bands using this method;

2) The higher order harmonic signals generated by the rectifier cannot be effectively rejected when the bandwidth of the network is larger than 2: 1 (e.g., $f_N > 2f_0$), which may reduce the overall power conversion efficiency of the rectenna.

To overcome the aforementioned drawbacks, the second type of multiband rectenna has been introduced and shown in Fig. 1(b). This rectenna is designed with multi-branch separate matching networks and rectifiers, where each branch is matched to a particular operating frequency. Meanwhile, the output DC power of the whole circuit is combined at the output

Manuscript receive October 30, 2017, revised March 05, 2018, accepted April 08, 2018. This work was supported in part by the EPSRC, U.K., and in part by the Aeternum LLC (*Corresponding author: Yi Huang*).

C. Song, Y. Huang, J. Zhou and S. Joseph are with the Department of Electrical Engineering and Electronics, University of Liverpool, Liverpool L69 3GJ, U.K. (e-mail: chaoyun.song@liv.ac.uk; yi.huang@ieee.org;).

P. Carter is with Global Wireless Solutions, Inc., Dulles, VA 20166 USA

G. Li is with College of Electronic Science and Engineering, National University of Defense Technology, Changsha 410073, China.

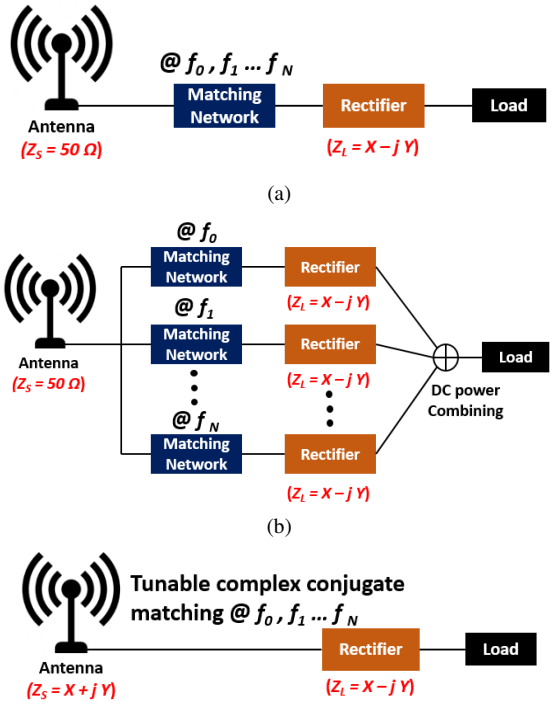

Fig. 1. (a) Configuration of a conventional rectifying antenna system with a single-branch impedance matching network. (b) Configuration of a rectifying antenna system with separate circuit branches. (c) The proposed novel frequency selectable rectenna without the need of impedance matching network.

port [21]-[26]. In this case, the loss of a single matching network can be reduced and the operating frequency of the rectenna can be extended by adding additional circuit branches. In this case, the harmonic signals of each single rectifier can also be effectively rejected. But, there are still disadvantages for this configuration. For example, the number of circuit components used for this configuration is normally very large and the structure of the design is quite complex (for a large frequency bandwidth). As a consequence, such rectennas would have a higher cost due to the complex fabrication process and structure.

In addition, the aforementioned conventional rectennas normally use antennas matched to standard 50 Ω. The matching networks should also match the complex high impedance of the rectifiers to 50 Ω as well. In this scenario, the performance of the rectenna would be very sensitive to the impedance variation of the nonlinear rectifier [19]. It is difficult to achieve consistent conversion efficiency in different operating conditions due to the impedance variation and mismatch.

In this paper, we introduce a novel design method for a wideband frequency selectable rectenna. An important feature is that the proposed rectenna does not require additional matching networks, which is very different from the existing rectennas. The antenna impedance (Zs) is directly (complex conjugate) matched with the rectifier impedance (Z_L) at several desired frequency bands, as shown in Fig. 1(c). Thus the proposed rectenna is of a relatively simple structure, a compact size and low cost. The frequency bands of interest can be easily tuned by loading a number of shorting pins on the antenna. Moreover, this novel design concept generates a high impedance complex conjugate matching system that could

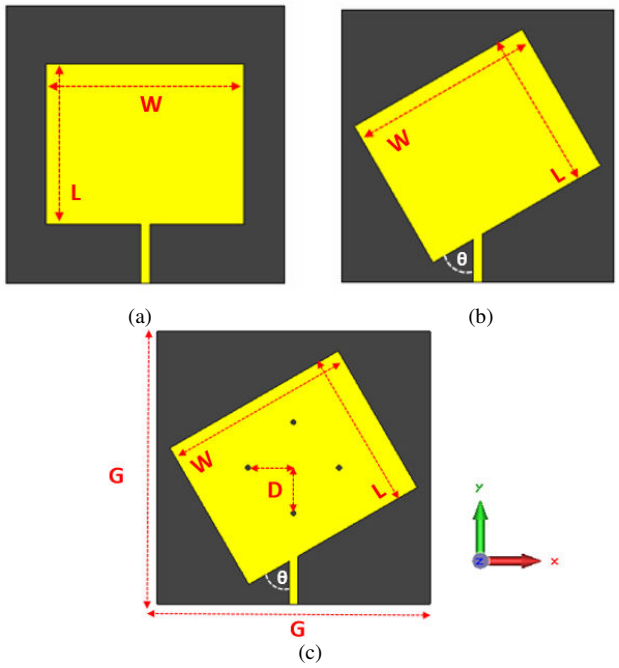

Fig. 2. (a) A typical center-fed microstrip patch antenna. (b) An off-center-fed patch antenna. (c) The proposed off-center-fed patch with shorting pins.

significantly reduce the performance variation due to the nonlinear effect of the rectenna, as discussed in [27]. The proposed rectenna is, therefore, suitable for a wide range of operating frequencies, input power levels and load impedance. To the authors' knowledge, it is the first time to introduce an "adaptive" rectenna with a wide selectable frequency band and consistent performance for different operating conditions, but without using complex matching circuits.

The rest of this paper is structured as follows. The detailed design steps are introduced in Section II and Section III. The measurement and experimental results are provided in Section IV. Finally, conclusions are drawn in Section V.

II. COMPACT RECTENNA DESIGN WITH SELECTABLE OPERATING FREQUENCY

A. *Multiband Matching Network Elimination*

The rectifiers are normally of complex high input impedance (e.g., real part > 200 Ω and |imaginary part| > 300 Ω) and their impedance is very sensitive to the variation of operating conditions (e.g., frequency, power and load) due to the strong nonlinearity of the rectifying diodes [23], [26]. Therefore, the design of the impedance matching network for broadband or multiband rectennas with consistent performance is extremely challenging. The reported rectenna designs in the literature are mostly based on the 50 Ω impedance matching system. Their matching networks are of complex structures, high cost and high loss. For an integrated rectenna design, if the antenna impedance can be tuned to the desired value, while the impedance of the antenna can directly conjugately match with that of the rectifier, the matching network of the complete rectenna is therefore eliminated. In this way, the design procedure is significantly simplified and the proposed rectenna is of a simple structure and low cost [27], [34]-[35].

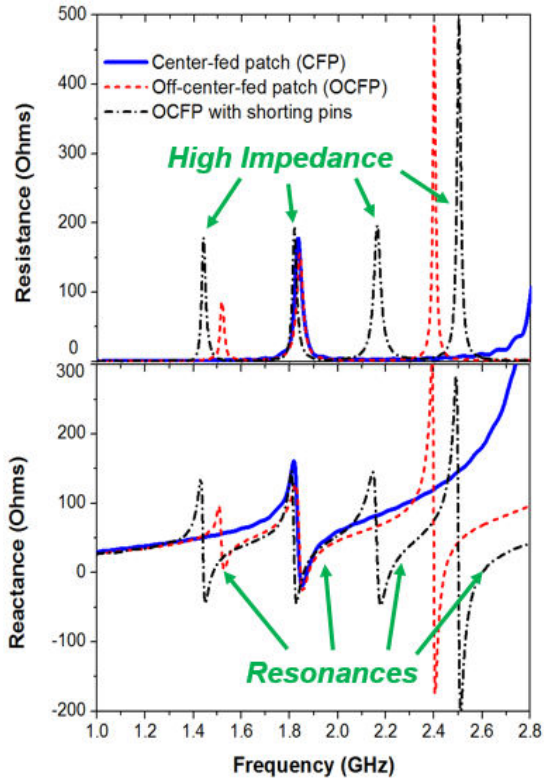

Fig. 3. The simulated real part (resistance) and imaginary part (reactance) of the impedance of center-fed patch (CFP) antenna, off-center-fed patch (OCFP) antenna, and the proposed OCFP with shorting pins.

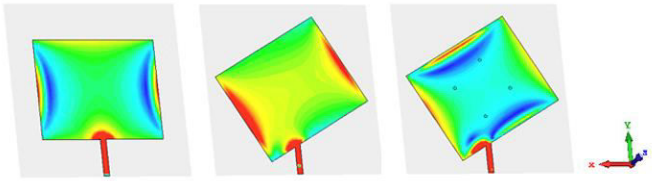

(a) (b) (c)

Fig. 4. The simulated surface current distributions at 1.85 GHz of (a) the center-fed patch (CFP) antenna; (b) the off-center-fed patch (OCFP) antenna; (c) the proposed OCFP with shorting pins.

Here, we propose a new method to manipulate the input impedance of a typical microstrip patch antenna, where the antenna impedance can be tuned to match with the impedance of the rectifier at the desired frequency band (with a ratio < 2: 1), and mismatch at other frequencies (for harmonic rejection). Using this method, we could get rid of the complex matching network of the conventional multiband and broadband rectenna, but the rectenna could still achieve competitive performance for the target applications (WPT and/or WEH).

The microstrip patch with a ground plane is one of the most common antennas. It has attractive features such as low cost, simple to design and easy to fabricate. As a design example, we employ such a patch antenna using Rogers Duroid5880 PCB with a relative permittivity of 2.2 and a thickness of 1.58 mm. As depicted in Fig. 2(a), the copper patch antenna on the top layer has a thickness of 70 μm and a size of $W \times L$ mm^2. The patch is fed by a typical microstrip line. The size of the PCB is $G \times G$ mm^2. From the theory [28], the radiating edges of the patch determine the resonant frequency of the antenna.

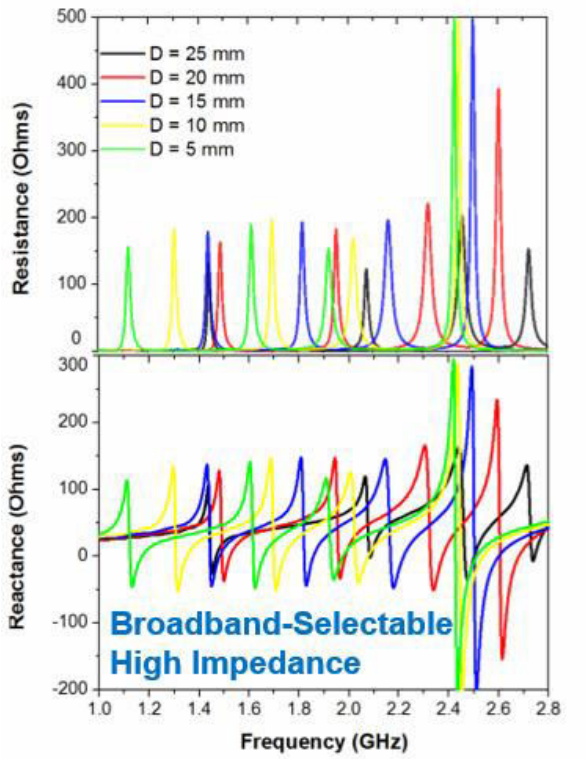

Fig. 5. The simulated real part (resistance) and imaginary part (reactance) of the proposed antenna with different values of parameter *D*.

Therefore, according to the design guide, if $W = 64$ mm, $L = 56$ mm and $G = 90$ mm, the fundamental resonant frequency of the patch antenna at TM_{100} mode is estimated as 1.84 GHz. The antenna performance is validated by using software simulations with the aid of the CST software. As shown in Fig. 3, the simulated real part (resistance) and imaginary part (reactance) of the antenna impedance show that a resonant frequency of the patch is indeed around 1.85 GHz (for resistance = 50 Ω and reactance = 0 Ω) which verifies the predictions. Additionally, the antenna also has anti-resonant performance at about 1.8 GHz, since the resistance is relatively high (e.g., about 200 Ω) while the reactance varies rapidly from 150 to -50 Ω at 1.8 GHz. In our case, the **anti-resonant high impedance of the antenna** would be used to directly conjugate match with the impedance of the rectifier. However, it is well known that a conventional microstrip center-fed-patch (CFP) antenna usually has a narrow frequency bandwidth. The ratio of the 2nd harmonic frequency/fundamental resonant frequency of the CFP is normally larger than 2. Consequently, if such CFPs are used for rectenna design without a matching network, the rectenna is only possible for a single narrow operating frequency band.

To adjust the frequency ratio of the CFP, we introduce a novel feeding method. As shown in Fig. 2(b), based on the geometric center of the patch, the antenna is rotated anti-clockwise by 90 – θ degrees. Thus the angle between the patch and the feed line is θ (θ = 60º in this example). In this case, the antenna is an off-center-fed patch (OCFP). The simulated surface current distributions of the CFP and OCFP at their fundamental resonant frequency (1.85 GHz) are compared

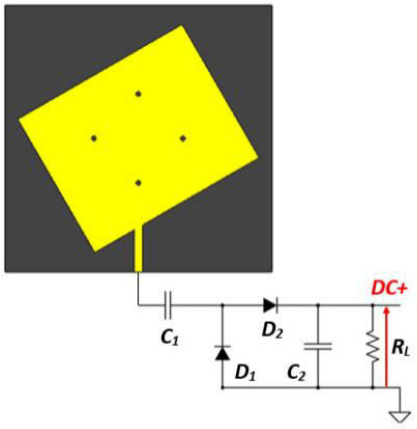

Fig. 6. The rectenna design using the proposed OCFP with shorting pins (D = 15 mm). The capacitors *C1* = *C2* = 100 nF, *D1* and *D2* are Schottky diodes HSMS2852, and R_L = 2000 Ω.

in Fig. 4. The OCFP shows stronger current flows on both sides of the radiating edges. In addition, the OCFP has a very strong current distribution on the edge that is close to the feed line, and has weaker current flows on other edges (see Fig. 4(b)). Due to this unbalanced current distribution, multiple resonant frequencies can be created between the fundamental and second resonant frequencies of the antenna [27]. From Fig. 3, it can be seen that the OCFP has realized three anti-resonant frequencies with relatively high impedance at around 1.5, 1.8 and 2.4 GHz over the frequency range of interest. Compared with the conventional CFP, the frequency ratio of the antenna is changed from 1: 2 (1.85 GHz/3.7 GHz) to about 1: 1.2 (1.5 GHz/1.8 GHz) which means more matching frequency points to large impedance.

Next, two pairs of identical shorting pins are symmetrically loaded on the OCFP with the aim to achieve selectable/flexible impedance matching for the rectenna design. The shorting pins are conducting holes which electrically connect the patch to the ground plane of the PCB. As depicted in Fig. 2(c), each hole has a diameter of 0.8 mm and a distance of *D* to the center of the PCB. The value of *D* in this figure is 15 mm as an example. Having loaded these shorting pins, from Fig. 4 it can be seen that the current has been suppressed to pass through the center area of the patch. The current distributions on the four edges of the patch are therefore enhanced. Compared with the CFP and OCFP, the proposed OCFP with shorting pins has produced an enhanced current flow on the top edge of the patch. Thus, additional resonant frequencies might be realized by combing the current paths at the top edge and two side edges of the patch. As shown in Fig. 3, the proposed OCFP with shorting pins has created an additional anti-resonant frequency around 2.15 GHz with a high impedance value of around 200 + j 150 Ω.

It is shown that, by modifying the conventional CFP to the proposed novel OCFP with shorting pins, the number of resonant/anti-resonant frequencies over the desired frequency band (with a frequency ratio < 2) is increased from one (at 1.85 GHz) to four (at around 1.45, 1.85, 2.15 and 2.45 GHz) over the band of interest. Multiband rectennas could therefore be designed using the proposed antenna without the need for matching networks.

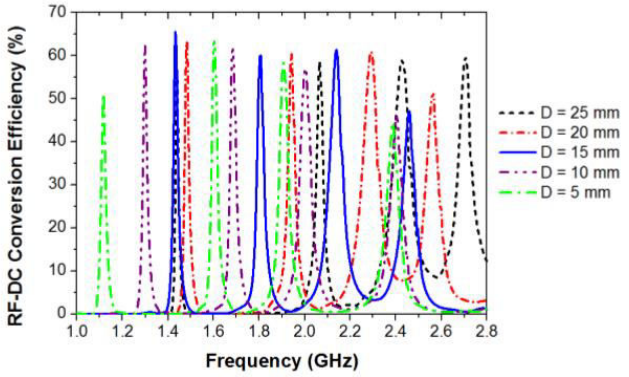

Fig. 7. The simulated RF-DC conversion efficiency of the proposed rectenna with different values of *D*. The received power by the rectenna is 0 dBm.

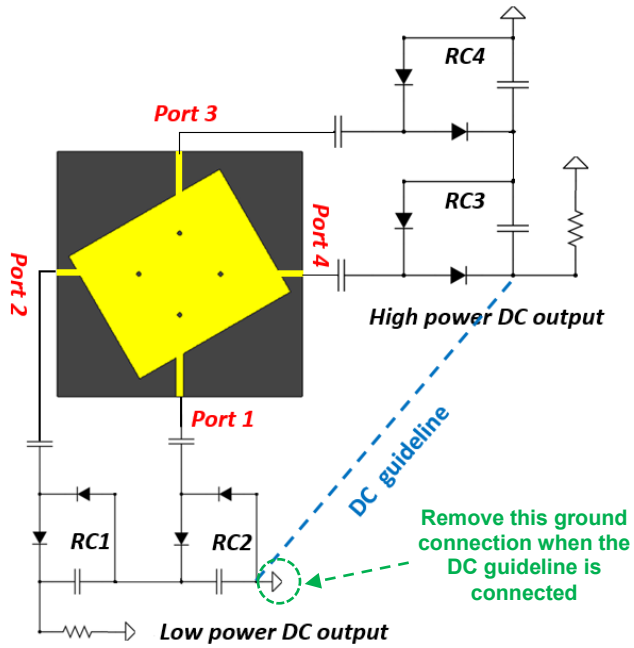

Fig. 8. The rectenna design for a wide input powers and load impedance range. The diodes are HSMS2852 for rectifying circuits RC1 and RC2, and are HSMS2862 for rectifying circuits RC3 and RC4. Note that the ground connection at RC2 should be disabled when the DC guideline is connected.

B. Broadband Frequency Selectable Design

In order to achieve a selectable operating frequency band for the proposed rectenna, the positions of the shorting pins can be tuned. According to the theory in [29], when the distance between the pins and the center of the patch is changed, the current strength on the edges and center areas of the patch will vary. As an example, we have studied the effects on the resonant frequency bands of the antenna by changing the value of *D*. The simulated resistance and reactance of the proposed antenna are shown in Fig. 5. It can be seen that the four resonant and anti-resonant frequency bands of the antenna are selectable from 1 to 2.8 GHz when the value of *D* is changed between 5 to 25 mm. Without modifying the physical dimension of the patch, the electrical size of the antenna is therefore selectable from 0.28 λ_0 to 0.78 λ_0 by changing the positions of the shorting pins.

The schematic view of the complete rectenna using the proposed OCFP with shorting pins is shown in Fig. 6. A typical

voltage doubler rectifier is selected due to its high conversion efficiency and simple topology [30]. The capacitors are typical 100 nF chip capacitors from Murata, the rectifying diodes are Schottky diode HSMS2852 from Avago and a typical 2000 Ω resistor is used as the load. The rectifier is directly connected to the antenna port without the introduction of any additional matching circuit components. The performance of the rectenna is co-simulated using the ADS and CST software. More specifically, a frequency domain power source is employed for the rectifier simulation using ADS, where the port impedance is directly linked to the antenna impedance exported from the CST.

Fig. 7 shows an example of simulated RF-DC conversion efficiency of the complete rectenna with different locations of the pins (parameter *D*). The efficiency is calculated using

$$\eta_{RF-DC} = \frac{P_{OUT}}{P_{IN}} \quad (1)$$

where P_{OUT} is the output DC power and P_{IN} is the received RF power by the antenna. In the simulation, P_{IN} is the input power of the frequency domain power source.

It can be seen that, when the input power is 1 mW (0 dBm), the rectenna is of high conversion efficiency (about 60%) at four different frequency bands. The frequency bands of the rectenna can be selected from 1.1 to 2.7 GHz by tuning the pin locations. It demonstrates that the proposed rectenna has selectable operating frequency over a broad band and also of high efficiency, the matching network of the rectenna is removed that would reduce the loss, cost and avoid fabrication errors (for a complex design).

III. Wide Power and Load Ranges Design

Another important feature is that the proposed rectenna is based on a high impedance conjugate matching system (i.e. both antenna and rectifier are of high impedance). Therefore, compared with conventional rectennas with a standard 50 Ω impedance system, the effect on the reflection coefficient of the rectenna caused by the impedance variation of the rectifier (due to the nonlinearity) is not very significant for the proposed system. Consequently, we may take advantage of this feature to make the proposed rectenna suitable for a wide input power and load impedance range without the introduction of additional matching circuit elements (which is normally a very complex procedure for conventional rectenna designs).

As shown in Fig. 8, based on the rectenna proposed in Section-II, three additional output ports are introduced for the OCFP antenna, ports 1 and 3 are orthogonal to ports 2 and 4. If we connect two identical rectifying circuits (*RC1* and *RC2*) to ports 1 and 2 respectively, and combine the output DC power of them, the rectenna is able to receive and rectify the incoming waves with random polarizations [31]. Similarly, this dual polarization capability is applied to ports 3 and 4 as well. To achieve a wide input power range, ports 1 and 2 are configured for low power DC output while port 3 and 4 are connected to the rectifiers for relatively high input powers. A DC guideline could be electrically connected between the low power and high power rectifiers.

As an example, the rectifying diodes of *RC1* and *RC2* are

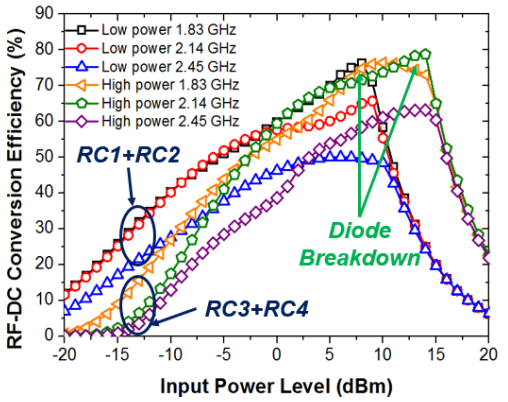

(a)

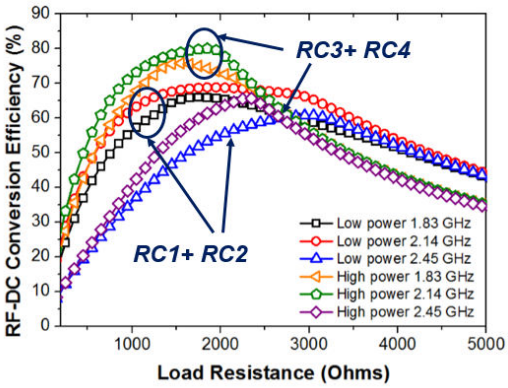

(b)

Fig. 9. The simulated RF-DC conversion efficiency vs. (a) input power level and (b) load resistance of the rectenna at three different frequency bands.

HSMS2852 with a forward bias voltage of 0.35 V and a breakdown voltage of 3.8 V, while the rectifying diodes of *RC3* and *RC4* are HSMS2862 with a forward bias voltage of 0.65 V and a breakdown voltage of 7 V [32]. Therefore, the rectifiers using the former diode (HSMS2852) would have a lower power consumption due to its smaller forward bias voltage, but the circuits would break down at a low input power level due to its smaller breakdown voltage. In contrast, the rectifier using the latter diode (HSMS2862) breaks down at higher input power levels but meanwhile has a higher consumption due to its larger forward bias and reverse breakdown voltages. In conventional rectenna designs, the impedance matching networks for rectifiers using different types of diodes are normally very different, since the packaging technologies and equivalent circuit models of the diodes are different [36], [37]. But, in our case, the proposed antenna may directly match well with the rectifiers using different diodes due to the high impedance system as discussed earlier.

The simulated RF-DC conversion efficiency of the proposed rectenna at three different frequency bands is shown in Figs. 9 (a) as a function of the input power level and (b) a function of the load resistance respectively. Here we test the low power and high power output ports separately (by disconnecting the DC guideline). A 2000 Ω load resistor is firstly used. From Fig. 9(a), it can be seen that the proposed high impedance antenna is well matched to the impedance of the rectifiers using two different types of diodes for the desired frequency bands around

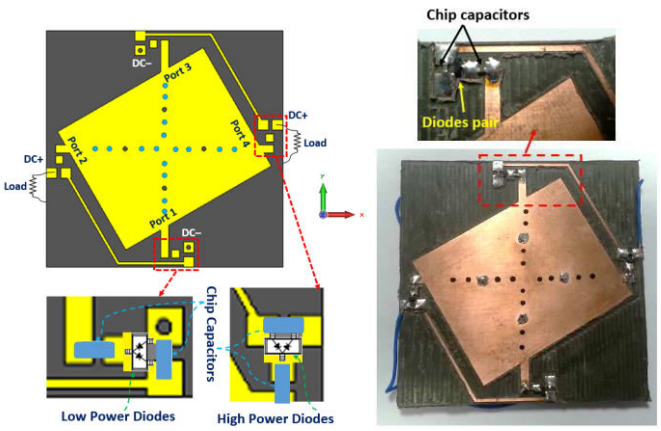

(a) (b)

Fig. 10. (a) The layout of the proposed frequency-reconfigurable adaptive rectenna. (b) The fabricated rectenna example.

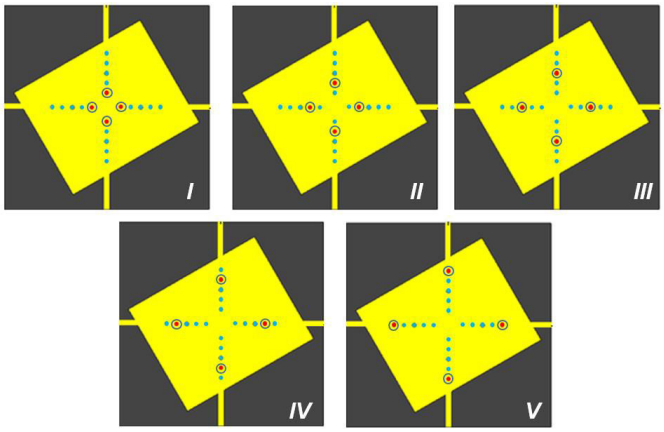

Fig. 11. Illustration of the shorting pins configuration for frequency reconfigurable design. The pins with electrical connections are highlighted by circles.

1.83, 2.14 and 2.45 GHz (for mobile, and Wi-Fi/ISM bands), since the conversion efficiency is relatively high in all cases. In addition, the conversion efficiency of the low power output port (*RC1* + *RC2*) is about 10% higher than that of the high power output port (*RC3* + *RC4*) when the input power is between -20 and 0 dBm. But, the low power rectifiers break down at the input power of 7 dBm with maximum conversion efficiency around 60 – 70%, while the high-power rectifiers break down at a higher input power level (around 14 dBm) with conversion efficiency up to 80%. At 0 dBm input power, the efficiency of the two-rectifier case as shown in Fig. 9 is a bit lower than that of the single rectifier case as depicted in Fig. 6. This is because that the rectifier impedance is slightly changed when the two rectifiers are connected. Therefore, it could slightly affect the conversion efficiency of the rectenna due to the impedance mismatch.

Next, by setting the input power to the optimal values (7 dBm for *RC1+RC2* and 14 dBm for *RC3+RC4*) for the rectifiers, the load resistance is changed from 100 to 5000 Ω. From Fig. 9(b), it can be seen that the conversion efficiency of the rectifiers at different frequency bands is nearly consistent over a wide range of load impedance. If we set conversion efficiency > 60% as a figure of merit, it is demonstrated that the proposed rectenna is adaptive for a wide input power range between 0 to 15 dBm, and for a wide load impedance range from 800 to 4000 Ω. The nonlinear effect of the rectifier is therefore significantly reduced which is of high significance for WPT and WEH used in practice.

It is demonstrated that this design is suitable for different types of rectifying diodes without the need of changing the impedance matching circuit: by substituting the presented diodes using other low power consumption diodes (e.g., heterojunction backward tunnel diodes [38]), better energy conversion efficiency could be achieved at lower input power levels (e.g., -30 to -10 dBm). The design presented in this paper is just an example to illustrate the proposed new idea. By following the design concept, the details of the rectenna could be modified to develop simple and compact rectennas that are suitable for any operating conditions without using complex matching circuits in the design.

TABLE I
OPERATING FREQUENCY OF THE RECTENNA FOR DIFFERENT CASES

	Parameter *D* (unit: mm)	Operating Frequency Band (unit: GHz)
Case I	5	1.1, 1.6, 1.9 and 2.4
Case II	10	1.3, 1.7, 2 and 2.4
Case III	15	1.4, 1.8, 2.1 and 2.5
Case IV	20	1.5, 1.9, 2.2 and 2.6
Case V	25	1.5, 2.1, 2.4 and 2.7

IV. EXPERIMENTAL RESULTS AND VALIDATIONS

The layout of the prototype rectenna is shown in Fig. 10 along with a picture of the fabricated example. The overall size of the PCB is 90 × 90 × 1.58 mm^3. It can be seen that the proposed rectenna is of a very simple structure with just a number of diodes and capacitors for the basic rectification, energy storage and output. No matching networks and extra circuit elements are added. Meanwhile, to realize the frequency reconfigurable feature, a series of holes are produced on the patch along the directions of horizontal and vertical feeding ports of the antenna. These holes are used to configure the shorting pins with different positions. By soldering or removing the electrical connections of the holes, the operating frequency band of the rectenna can be manually tuned by changing the distance (parameter *D*) between the shorting pins and patch center. As depicted in Fig. 11, there are five different scenarios for the configurations of shorting pins, which are *D* = 5, 10, 15, 20 and 25 mm respectively. According to Fig. 7, the operating frequency band of the rectenna for these five cases are given in Table I. In this way, the rectenna can achieve a wide selectable frequency band from 1.1 to 2.7 GHz

As a design example, the shorting pins on the patch as shown in Figs. 10 (a) and (b) were configured for the *Case III*

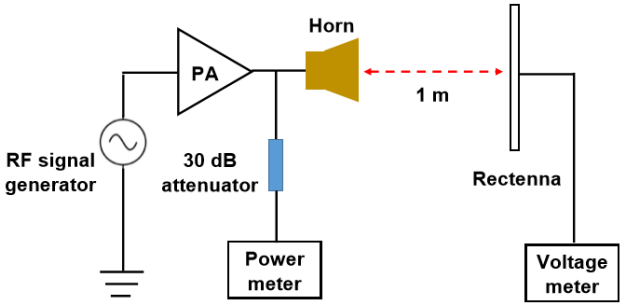

Fig. 12. The measurement setup of the proposed rectenna. The rectenna direction is tuned to match with its maximum gain direction.

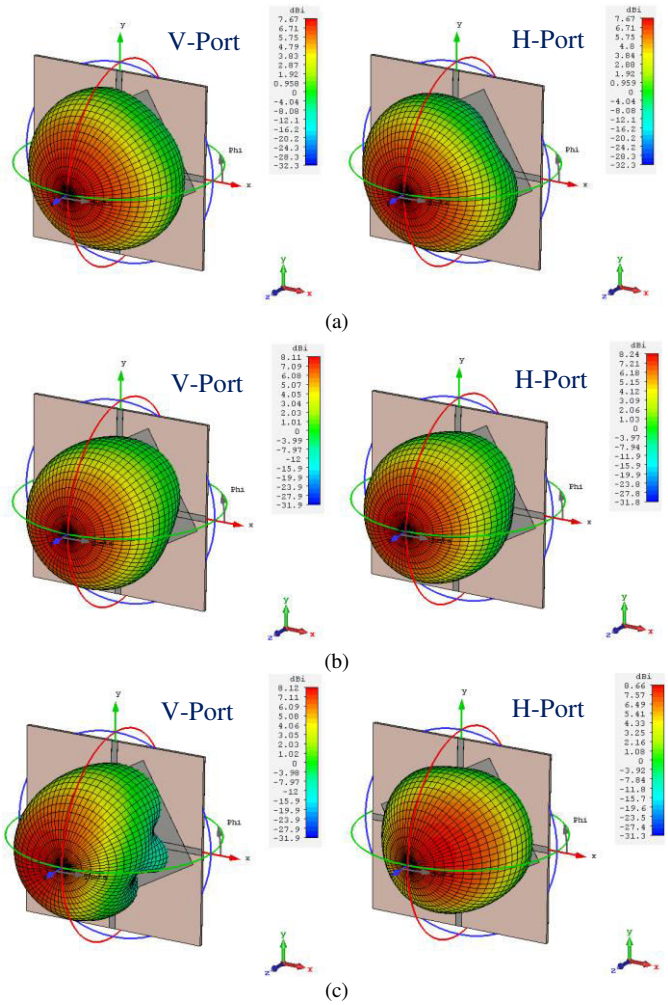

Fig. 13. The simulated 3D radiation patterns (with directivities) of the proposed rectenna for the vertical-port (ports 1 and 3) and horizontal-port (ports 2 and 4) at (a) 1.83 GHz (b) 2.14 GHz and (c) 2.45 GHz.

where its operating frequency bands were of around 1.4, 1.8, 2.1 and 2.45 GHz (D = 15 mm in this case). It is also noted that the high power and low power rectifiers were connected by the DC guideline (the ground connection at *RC2* was disabled in this case, as shown in Fig. 8). Thus there was only one output port for the measurement of DC power in this example.

The measurement setup of the rectenna is shown in Fig. 12. The signals generated by an RF signal generator were amplified by using a 30 dB gain power amplifier (PA), and transmitted by

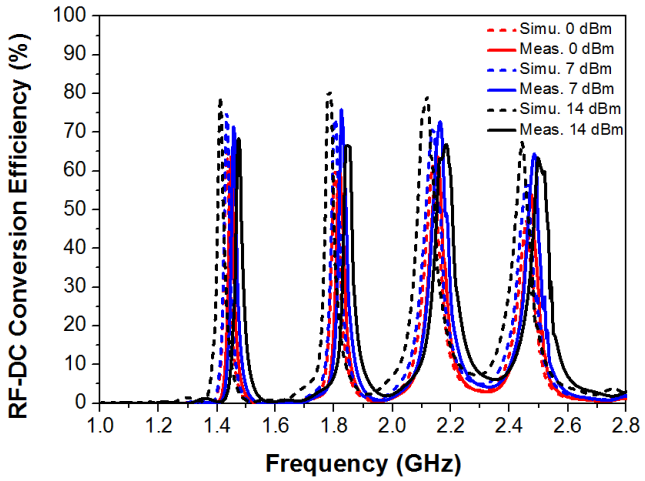

Fig. 14. The simulated and measured conversion efficiency vs. frequency at three different input power levels. The load resistance is 2000 Ω.

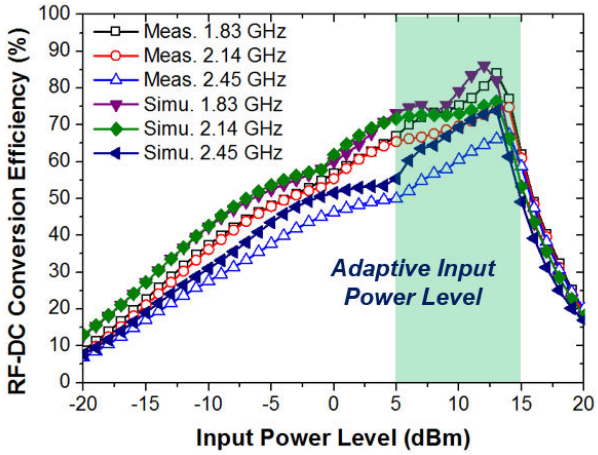

Fig. 15. The simulated and measured conversion efficiency vs. input power level at three different frequency bands. The load resistance is 2000 Ω.

TABLE II
SIMULATED RADIATION EFFICIENCY OF THE ANTENNA

Frequency	Port	Radiation Efficiency (CST simulated)
1.83 GHz	V-Port	92.3%
	H-Port	95.6%
2.14 GHz	V-Port	94.9%
	H-Port	97.1%
2.45 GHz	V-Port	80.7%
	H-Port	82.5%

a calibrated horn antenna R&SHF906. The proposed rectenna was used to receive the signals with a distance of 1 m from the transmitting horn antenna. The transmitting power was measured by using a power meter while the received power by the rectenna was calculated by using the Friis transmission equation [33].

$$P_r = P_t + G_t + G_r + 20\log_{10}\frac{\lambda}{4\pi r} \quad (2)$$

where P_r is the received power in dBm, P_t is the transmitting power of the horn in dBm, G_t is the realized gain of the horn in dBi, G_r is the realized gain of the proposed rectenna in dBi, λ is

TABLE III
COMPARISON OF THE PROPOSED RECTENNA AND RELATED DESIGNS

Ref. (year)	Operating Frequency (GHz)	Complexity of the overall design	Maximum RF-DC conversion efficiency (%)	Input power level (IPL) and load impedance range (LIR) for conversion efficiency > 60%	Summary of the key features
[17] (2014)	Single-band 2.45	Very complex	75 at 19 dBm	IPL: 16 – 20 dBm LIR: 100 – 5000 Ω	Buck-boost converter as the load to improve the rectifier linearity
[18] (2015)	Reconfigurable 5.2, 5.8	Very complex	70 at 16.5 dBm	IPL: 12 – 18 dBm LIR: 150 Ω	Use switches in the matching network for reconfigurable frequency band
[22] (2015)	Dual-band 0.915, 2.45	Complex	70 at 0 dBm	IPL: -5 – 3 dBm LIR: 500 – 3000 Ω	Resistance compression matching network for improving the rectifier linearity
[23] (2015)	Four-band 0.9, 1.8, 2.1, 2.4	Very complex	84 at 0 dBm	IPL: -10 – 0 dBm LIR: 11000 Ω	Stacked rectifier arrays for multiband energy harvesting
[24] (2012)	Tunable 0.9 – 2.45	Very complex	80 at 30 dBm	IPL: Tunable 8 – 30 dBm LIR: 750 Ω	Switchable adaptive rectifier arrays for a wide input power range
[26] (2016)	Six-band 0.55, 0.75, 0.9, 1.85, 2.15, 2.45	Very complex	80 at -3 dBm	IPL: -15 – 0 dBm LIR: 10 – 80 kΩ	Improved impedance matching networks for consistent conversion efficiency
[27] (2016)	Broad-band 0.9 – 1.1, 1.8 – 2.5	Simple	75 at 20 dBm	IPL: Tunable 0 – 23 dBm LIR: 200 – 2000 Ω	Broadband high impedance conjugate matching without additional matching circuits
This work (2017)	**Selectable 1.1 – 2.7**	**Simplest**	**85 at 12 dBm**	**IPL: 0 – 15 dBm** **LIR: 700 – 4500 Ω**	**Selectable broadband, adaptive input power and load impedance range, no matching circuits**

the wavelength of interest, and r is the distance (r = 1 m). Since the antenna has been integrated with the rectifier, the realized gain of the rectenna cannot be measured with a typical 50 Ω port. The realized gain was calculated using the directivity of the antenna multiples the radiation efficiency of the antenna (simulated using the CST) and impedance matching efficiency of the complete rectenna (obtained from the ADS). An example of the simulated 3D radiation patterns (for the vertical ports 1 & 3 and horizontal ports 2 & 4) of the proposed rectenna is shown in Fig. 13 at the frequency bands of interest. The antenna is linearly polarized over the V- and H-ports, while the maximum radiation fields at 1.83 and 2.14 GHz are realized at the boresight direction of the antenna. The maximum radiation beam of the antenna is slightly tilted at 2.45 GHz. In this case, the antenna direction should be tuned in the measurement in order to match with its maximum radiation directions. According to Fig. 13, it can be seen that the maximum gains of the antenna for all ports are about 7.47, 8.24 and 8.66 dBi at 1.83, 2.14 and 2.45 GHz respectively. Moreover, the corresponding simulated antenna radiation efficiency at these frequencies is given in Table II for the vertical and horizontal ports. The efficiency is over 80% for all cases.

The simulated and measured conversion efficiency of the proposed rectenna example (as shown in Fig. 10) are given in Fig. 14. It can be seen that the rectenna has high efficiency (e.g., over 60%) at four different frequency bands (around 1.45, 1.83, 2.15 and 2.45 GHz) with about a 40–50 MHz bandwidth of each. The efficiency is almost maintained for three different power levels (from 0 to 14 dBm). If the efficiency is studied as a function of the input power level, as depicted in Fig. 15, the efficiency is always higher than 60% for the input power between 0 and 15 dBm. The maximum conversion efficiency is achieved at the input power level of around 12 dBm.

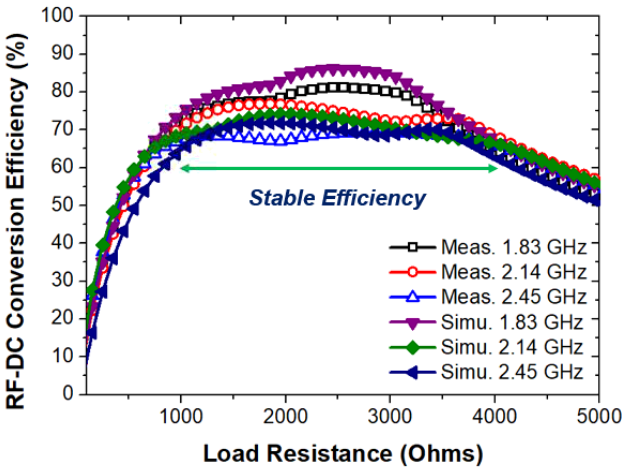

Fig. 16. The simulated and measured conversion efficiency vs. load resistance at three different frequency bands. The input power level is 12 dBm.

The maximum efficiency is about 85% at 1.83 GHz, 75% at 2.14 GHz and 70% at 2.45 GHz respectively. Next, the input power is fixed at the optimal value (12 dBm), and the conversion efficiency is measured versus a range of load impedance, as shown in Fig. 16. It can be seen that, at the desired frequency bands, the conversion efficiency is constantly high (over 60%) over a large load impedance range from 700 to 4500 Ω. The above results have shown good agreements between the simulation and measurement due to the simplified structure and fabrication process of this design.

A comparison between the proposed rectenna using the novel design method and other related work reported in the literature is given in Table III. Our rectenna has a very wide selectable frequency band with relatively high conversion

efficiency (up to 85%). Compared with other work that uses buck-boost converter [17], resistance compression network [22] and switchable adaptive rectifier arrays [24] etc. for reducing the nonlinearity of the system, our rectenna has demonstrated an improved circuit linearity with consistent efficiency over a wide input power and load impedance range. But, our rectenna does not need the complex matching networks or circuit elements; thus, it has the simplest structure for the rectennas with the similar performance. Moreover, it should be noted that the presented design is different from our previous work in [27]. In the previous work, we demonstrated a method of tuning the impedance value of a broadband dipole antenna in order to get it matched with the rectifier impedance directly, which could be considered as a design guide for broadband rectennas. This work introduces a new method of developing the rectenna from a single narrowband patch antenna to a multiband device without the need of impedance matching networks. This design could be a good example for simplified multiband rectennas. In addition, the conventional multiband and broadband rectenna designs normally require a complex software optimization procedure (for tuning the matching circuit components). The proposed new method is relatively simple without the selection of circuit elements hence is of great significance for volume production of such rectennas in practice.

V. Conclusion

A new design method for an adaptive rectenna with a wide selectable frequency band has been presented. The proposed rectenna using this design method has achieved more than 60% energy conversion efficiency at four frequency bands that are selectable from 1.1 to 2.7 GHz, and over a wide input power range from 0 to 15 dBm and a wide load impedance range from 700 to 4500 Ω. The most attractive feature is that the proposed rectenna does not need a complex impedance matching network, thus the rectenna can be of a compact size, a simple structure and low cost. It has shown excellent performance for the target WPT and WEH applications. The design concept is easy to follow and of great significance for the real production of rectennas with simplified structures and reduced costs.

References

[1] J. Garnica, R. A. Chinga, and J. Lin, "Wireless power transmission: From far-field to near-field," *Proc. IEEE*, vol. 101, no. 6, pp. 1321–1331, Jun. 2013.

[2] X. Lu, P. Wang, D. Niyato, D. I. Kim, and Z. Han, "Wireless charging technologies: Fundamentals, standards, and network applications," *IEEE Commu. Surveys Tutos.*, vol. 18, no. 2, pp. 1413–1452, 2nd Quart. 2016.

[3] M. Ettorre, W. A. Alomar and A. Grbic, "Radiative wireless power-transfer system using wideband, wide-angle slot arrays," *IEEE Trans. on Antennas and Propag*., vol. 65, no. 6, pp. 2975-2982, Jun. 2017.

[4] W. Li and C. Mi, "Integrated *LCC* compensation topology for wireless charger in electric and plug-in electric vehicles," *IEEE Trans. Ind. Electron.*, vol. 62, no. 7, pp. 4215–4225, Jul. 2015.

[5] G. Buja, M. Bertoluzzo and K. N. Mude : "Design and experimentation of WPT charger for electric city car", *IEEE Trans. Power Electron,*, vol. 62, no. 12, pp. 7436–7447, Dec. 2015.

[6] C. H. Ou, H. Liang, and W. Zhuang, "Investigating wireless charging and mobility of electric vehicles on electricity market," *IEEE Trans. Ind. Electron.*, vol. 62, no. 5, pp. 3123–3133, May 2015.

[7] S. Y. R. Hui, W. Zhong, and C. K. Lee, "A critical review of recent progress in mid-range wireless power transfer," *IEEE Trans. Power Electron.*, vol. 29, no. 9, pp. 4500–4511, Sep. 2014.

[8] A. A. Nasir, X. Zhou, S. Durrani and R. A. Kennedy, "Relaying protocols for wireless energy harvesting and information processing," *IEEE Trans. Wireless Communications*, vol. 12, no. 7, pp. 3622-3636, Jul. 2013.

[9] V. C. Gungor and G. P. Hancke, "Industrial wireless sensor networks: Challenges, design principles, and technical approaches," *IEEE Trans. Ind. Electron.*, vol. 56, no. 10, pp. 4258–4265, Oct. 2009.

[10] R. Colella, L. Tarricone, L. Catarinucci, "SPARTACUS: Self-powered augmented RFID tag for autonomous computing and ubiquitous sensing," *IEEE Trans. on Antennas and Propag.*, vol.63, no.5, pp.2272-2281, May 2015

[11] M. Fantuzzi, D. Masotti, and A. Costanzo, "A novel integrated UWB UHF one-port antenna for localization and energy harvesting," *IEEE Trans. Antennas Propag.*, vol. 63, no. 9, pp. 3839–3848, Sep. 2015.

[12] Y. Cao, T. Jiang and Z. Han, "A survey of emerging M2M systems: context, task, and objective," *IEEE Internet Things J.*, vol. 3, No. 6, pp. 1246-1258, Jun. 2016.

[13] L. Catarinucci et al., "An IoT-aware architecture for smart healthcare systems," *IEEE Internet Things J*., vol. 2, No. 6, pp. 515-526, Mar. 2015.

[14] H. J. Visser and R. J. M. Vullers, "RF energy harvesting and transport for wireless sensor network applications: Principles and requirements," *Proc. IEEE*, vol. 101, no. 6, pp. 1410–1423, Jun. 2013.

[15] A. Costanzo et al., "Electromagnetic energy harvesting and wireless power transmission: A unified approach," *Proc. IEEE*, vol. 102, no. 11, pp. 1692–1711, Nov. 2014.

[16] J. Colomer-Farrarons, P. Miribel-Català, A. Saiz-Vela, and J. Samitier "A multiharvested self-powered system in a low-voltage low-power technology," *IEEE Trans. Ind. Electron.*, vol. 58, no. 9, pp. 4250–4263, Sep. 2011.

[17] Y. Huang, N. Shinohara, and T. Mitani, "A constant efficiency of rectifying circuit in an extremely wide load range," *IEEE Trans. Microw. Theory Tech.*, vol. 62, no. 4, pp. 986–993, Apr. 2014.

[18] P. Lu, X. Yang, J. Li, and B. Wang, "A compact frequency reconfigurable rectenna for 5.2- and 5.8-GHz wireless power transmission," *IEEE Trans. Power Electron.*, vol. 30, no. 11, pp. 6006–6010, Nov. 2015.

[19] Y. Han, O. Leitermann, D. A. Jackson, J. M. Rivas, and D. J. Perreault, "Resistance compression networks for radio-frequency power conversion," *IEEE Trans. Power Electron.*, vol. 22, no. 1, pp. 41–53, Jan. 2007.

[20] T. Paing, J. Shin, R. Zane, and Z. Popovic, "Resistor emulation approach to low-power RF energy harvesting," *IEEE Trans. Power Electron*., vol. 23, no. 3, pp. 1494–1501, Mar. 2008.

[21] C. Song, Y. Huang, J. Zhou and P. Carter, "Improved ultra-wideband rectennas using hybrid resistance compression technique," *IEEE Trans. Antennas Propag.*, vol. 65, no. 4, pp. 2057–2062, Apr. 2017.

[22] K. Niotaki, A. Georgiadis, A. Collado, and J. S. Vardakas, "Dual-band resistance compression networks for improved rectifier performance," *IEEE Trans. Microw. Theory Tech.*, vol. 62, no. 12, pp. 3512–3521, Nov. 2015.

[23] V. Kuhn, C. Lahuec, F. Seguin, and C. Person, "A multi-band stacked RF energy harvester with rf-to-dc efficiency up to 84%," *IEEE Trans. Microw. Theory Tech.*, vol. 63, no. 5, pp. 1768–1778, May 2015.

[24] V. Marian, B. Allard, C. Vollaire, and J. Verdier, "Strategy for microwave energy harvesting from ambient field or a feeding source," *IEEE Trans. Power Electron*., vol. 27, no. 11, pp. 4481–4491, Nov. 2012.

[25] C. Song, Y. Huang, J. Zhou, J. Zhang, S. Yuan and P. Carter, "A high-efficiency broadband rectenna for ambient wireless energy harvesting," *IEEE Trans. Antennas Propag.*, vol. 63, no. 8, pp. 3486–3495, May 2015.

[26] C. Song, et al, "A novel six-band dual CP rectenna using improved impedance matching technique for ambient RF energy harvesting," *IEEE Trans. Antennas Propag*., vol. 64, no. 7, pp. 3160–3171, Jul. 2016.

[27] C. Song, et al, "Matching network elimination in broadband rectennas for high-efficiency wireless power transfer and energy harvesting," *IEEE Trans. Ind. Electro.*, vol. 64, no. 5, pp. 3950–3961, Apr. 2017.

[28] Y. Huang and K. Boyle, *Antennas: From Theory to Practice*. Hoboken, NJ: Wiley, 2008.

[29] X. Zhang and L. Zhu, "Patch antennas with loading of a pair of shorting pins towards flexible impedance matching and low cross polarization," *IEEE Trans. Antennas Propag*., vol. 64, no. 4, pp. 1226–1233, Apr. 2016.

[30] J. P. Curty, N. Joehl, F. Krummenacher, C. Dehollain, and M. J. Declercq, c"A model for u-power rectifier analysis and design," *IEEE Trans. Circuits Syst. I, Reg. Papers*, vol. 52, no. 12, pp. 2771–2779, Dec. 2005.

[31] J.-h. Chou, D.-b. Lin, K.-l. Weng and H.-j. Li, "All polarization receiving rectenna with harmonic rejection property for wireless power

transmission," *IEEE Trans. Antennas and Propag.*, vol. 62, no. 10, pp. 5242–5249, Oct. 2014.
[32] *HSMS-285x, HSMS-286x Surface Mount Microwave Schottky Detector Diodes*, Data Sheet. Avago Technologies, Inc., San Jose, CA, USA, 2015.
[33] S. Ladan, A. B. Guntupalli, and K. Wu, "A high-efficiency 24 GHz rectenna development towards millimeter-wave energy harvesting and wireless power transmission," *IEEE Trans. Circuits Syst. I, Reg. Papers*, vol. 61, no. 12, pp. 3358–3366, Dec. 2014.
[34] H. J. Visser, S. Keyrouz and A. B. Smolders, "Optimized rectenna design", *Wireless Power Transfer*, vol. 2, no. 1, pp. 44–50, Mar. 2015.
[35] H. Sun, Y.-X. Guo, M. He, and Z. Zhong, "Design of a high-efficiency 2.45-GHz rectenna for low-input-power energy harvesting," *IEEE Antennas Wireless Propag. Lett.,* vol. 11, pp. 929–932, 2012.
[36] H. Sakaki et al., "A novel wide dynamic range rectifier design for wireless Power Transfer system," in *2014 Asia-Pacific Microwave Conference*, Sendai, Japan, 2014, pp. 1208-1210.
[37] H. Sun, Z. Zhong, and Y.-X. Guo, "An adaptive reconfigurable rectifier for wireless power transmission," *IEEE Microw. Wireless Compon. Lett*., vol. 23, no. 9, pp. 492–494, Sep. 2013.
[38] C. H. P. Lorenz et al., "Breaking the efficiency barrier for ambient microwave power harvesting with heterojunction backward tunnel diodes," *IEEE Trans. Microw. Theory Techn.,* vol. 63, no. 12, pp. 4544–4555, Dec. 2015.

Chaoyun Song (S'16–M'17) received the B.Eng. (Hons.) degree in telecommunication engineering from Xi'an Jiaotong-Liverpool University, Suzhou, China, in 2012, and the M.Sc. degree and PhD degree with distinctions in electrical engineering and electronics from The University of Liverpool (UoL), Liverpool, U.K., in 2013 and 2017 respectively.

He previously worked as a Research Assistant and Antenna Design Engineer at the UoL and BAE systems, Chelmsford, UK during 2015-2016. He is currently a Postdoctoral Research Associate at the High Frequency Engineering Research Group of the University of Liverpool, UK. Dr. Song has authored/co-authored more than 25 papers in internationally refereed journals and conference proceedings. He has also filed 5 US and UK patents. He was the receipts of many international awards such as the winner of the IET Present Around the World Competition (2016) and the EM Bright-Sparks Award for outstanding young (under age 30) electronic engineers in the UK (2018). He won the BAE Systems Chairman's Award in 2017 for the innovation of next generation GNSS antennas.

His current research interests include liquid antennas, novel materials, wireless energy harvesting, rectifying antennas, circular polarization antenna, power management circuit, wireless power transfer, GNSS and anti-jamming technologies and smart sensors for the IoT. Dr. Song has been a regular reviewer of 10 international journals including Applied Physics Letters, Scientific Reports, IEEE Transactions on Antennas and Propagation, IEEE Transactions on Industrial Electronics, IEEE Transactions on Microwave Theory and Techniques, IEEE Transaction on Circuits and Systems I: Regular Papers, IEEE Antennas and Wireless Propagation Letters and IEEE Sensors letters.

Yi Huang (S'91–M'96–SM'06) received the B.Sc. degree in physics from Wuhan University, Wuhan, China, in 1984, the M.Sc.(Eng.) degree in microwave engineering NRIET, Nanjing, China, in 1987, and the D.Phil. degree in communications from the University of Oxford, Oxford, U.K., in 1994.He has been conducting research in the areas of wireless communications, applied electromagnetics, radar, and antennas since 1987. He was with NRIET, as a Radar Engineer and spent various periods with the Universities of Birmingham, Oxford, and Essex, U.K. as a Member of Research Staff. In 1994, he joined British Telecom Labs, as a Research Fellow. In 1995, he joined the Department of Electrical Engineering and Electronics, University of Liverpool, Liverpool, U.K., as a faculty member, where he is currently a Full Professor in Wireless Engineering, the Head of the High Frequency Engineering Group and Deputy Head of Department. He has authored over 300 refereed papers in leading international journals and conference proceedings, and authored Antennas: From Theory to Practice (Wiley, 2008) and Reverberation Chambers: Theory and Applications to EMC and Antenna Measurements (Wiley, 2016).Prof. Huang is a Senior Fellow of the HEA. He is a Fellow of the IET. He has received many research grants from research councils, government agencies, charity, EU and industry, acted as a consultant to various companies, and served on a number of the national and international technical committees and has been an Editor, Associate Editor, or Guest Editor of four international journals. He has been a keynote/invited speaker and organizer of many conferences and workshops (e.g., WiCom 2006, 2010, IEEE iWAT2010, and LAPC2012). He is currently the Editor-in-Chief of Wireless Engineering and Technology, Associate Editor of IEEE Antennas and Wireless Propagation Letters, U.K., and Ireland Rep to the European Association of Antenna and Propagation (EurAAP).

Paul Carter received the B.Sc. degree (Hons.) in physics from the University of Manchester, U.K., in 1987, the M.Sc. degree (Eng.) in microelectronic systems and telecommunications, in 1988, and the Ph.D. degree in electrical engineering and electronics, in 1991 both from the University of Liverpool, U.K.

He is the President and CEO of Global Wireless Solutions, Inc. (GWS), Dulles, VA, USA, a leading independent benchmarking solution vendor for the wireless industry. With more than 25 years of experience in the cellular network industry, he founded Global Wireless Solutions to provide operators with access to in-depth, accurate network benchmarking, analysis, and testing. Prior to GWS, he directed business development and CDMA engineering efforts for LLC, the world's largest independent wireless engineering company.

Jiafeng Zhou received the B.Sc. degree in radio physics from Nanjing University, Nanjing, China, in 1997, and the Ph.D. degree from the University of Birmingham, Birmingham, U.K., in 2004. His Ph.D. research concerned high-temperature superconductor microwave filters.

He was with the National Meteorological Satellite Centre of China, Beijing, China, from 1997, for two and a half years, where he was involved in the development of communication systems for Chinese geostationary meteorological satellites. From 2004 to 2006, he was a Research Fellow with the University of Birmingham, where he was involved in phased arrays for reflector observing systems. He then moved to the Department of Electronic and Electrical Engineering, University of Bristol, Bristol, U.K., until 2013, where he was involved in the development of highly efficient and linear amplifiers. He is currently with the Department of Electrical Engineering and Electronics, The University of Liverpool, Liverpool, U.K. His current research interests include microwave power amplifiers, filters, electromagnetic energy harvesting, and wireless power transfer.

Sumin David Joseph received the B.Tech degree (Hons.) in Electronics & Communication from Cochin University of Science and Technology, India in 2012. He received his M.Tech degree (Hons.) in Communication Systems from Visvesvaraya National Institute of Technology, India in 2015. He is currently working towards a dual Ph.D. degree in electrical engineering at the University of Liverpool, U.K and National Tsing Hua University, Taiwan.

He worked as a lab engineer under CoE at Visvesvaraya National Institute of Technology,

India where he was involved in projects of national importance. His research interests include self-biased circulators, mm-wave antenna arrays, rectifying antennas, rectifiers, wireless power transfer and energy harvesting.

Gaosheng Li (M'08) received his B.S. degree in electromagnetic field and microwave and his M.S. degree as well as his PH. D. in electronic science and technology from the National University of Defense Technology (NUDT), Changsha, China, in 2002, 2004 and 2013, respectively.

He has been with NUDT as a Teaching Assistant from 2004 to 2006, and a Lecturer from 2006 to 2011, and then as an Associate Professor since 2011. From 2014 to 2016, he was with Nanjing University of Aeronautics and Astronautics (NUAA) and Wuxi Huace Electronic Systems Co., Ltd., China as a Postdoctoral Research FellowFrom 2016 to 2017, he is a Visiting Scholar at the University of Liverpool (UoL), United Kingdom, sponsored by China Scholarship Council (CSC). His research interests include Antennas and Propagation (AP), Electromagnetic Compatibility (EMC), Wireless Propagation and Microwave Systems.

Dr. Li is the author or coauthor of 6 books and 99 papers published in journals and conference proceedings. He owns 21 Chinese patents and 6 software copyrights. He won 2 national scientific prizes in 2007 and 2013, respectively. He is a Member (2008) of the IEEE AP Society and EMC Society, a Member (2016) of IET, a Member (2017) of ACES, and a Member (2011) of the Institute of Electronics, Information and Communication Engineers (IEICE), as well as a Senior Member (M'2008, SM'2014) of the Chinese Institute of Electronics (CIE).